ACS APPLIED MATERIALS & INTERFACES

Research Article

www.acsami.org

Glucose Sensor using Liquid-Crystal Droplets Made by Microfluidics

Jiyeon Kim,[†,‡] Mashooq Khan,[†,‡] and Soo-Young Park*[,†]

[†]Department of Polymer Science and Engineering, Kyunpook National University, #1370 Sangyuk-dong, Buk-gu, Daegu 702-701, Korea

Supporting Information

ABSTRACT: Micrometer-sized, 4-cyno-4-pentylbiphenyl (5CB) droplets were developed for glucose detection in an aqueous medium by coating with poly(acrylicacid-*b*-4-cynobiphenyl-4-oxyundecylacrylate) (PAA-*b*-LCP) at the 5CB/water interface and covalently immobilizing glucose oxidase (GOx) to the PAA chains. This functionalized liquid-crystal (LC) droplet detected glucose from a radial to bipolar configurational change by polarized optical microscopy under crossed polarizers at concentrations as low as 0.03 mM and response times of ∼3 min and showed the selective detection of glucose against galactose. This new and sensitive LC-droplet-based glucose biosensor has the merits of low production cost and easy detection by the naked eye and might be useful for prescreening the glucose level in the human body.

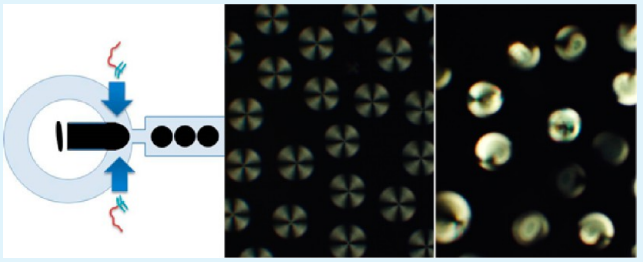

KEYWORDS: *biosensor, glucose, GOx, 5CB, droplets, liquid crystal*

1. INTRODUCTION

Glucose is a primary source of energy for the body's cells. The normal blood glucose level (BGL) ranges from 3.5 to 6 mM. A BGL higher than 11 mM leads to hyperglycemia, which causes several complications, such as dry skin, extreme thirst, blurred vision, drowsiness, and slow wound healing.[1] These symptoms may not be noticeable until the BGL value reaches 15−20 mM, which can lead to potential life-threatening diabetic ketoacidosis (DKA) or diabetic coma. DKA occurs most frequently in those who already have diabetes, or it might be the first symptom in someone who was not previously diabetic.[2] Sometimes an abnormally low BGL causes hypoglycemia, which can produce a range of complications, such as neuroglycopenia, dysphoria, serious seizures, unconsciousness, and permanent brain damage.[3] All of these complications can be avoided if hypoglycemia is identified at the early stages. In this regard, biosensors allow the medical field to leverage the diagnosis to monitor the BGL on a daily basis. Measuring techniques, such as the luminescence, spectroscopy, chromatography, and electrochemical analysis, are available to screen the BGL, but a number of obstacles, such as ion interference, high cost, and slow and unreliable detection, still need to be resolved.

Over the last decade, liquid crystals (LCs) have been used to develop innovative biosensors for bedside diagnosis and laboratory applications. LCs with high birefringence and extreme sensitivity to the surface interactions at the LC/aqueous interface can eliminate the need for markers, tags, and so forth in the biosensors for label-free detection.[4] LC biosensors rely on the interactions between sensing a LC medium and the specimen of interest at the interface. The responses of LCs in the presence of a synthetic polymer,[5−7] endotoxine,[8] surfactants,[9,10] proteins,[11−13] and simple electrolytes[14] at the LC/water interface have been reported. Moreover, when a specimen consists of pH-sensitive functional groups, the orientations of LCs become sensitive to the pH in the aqueous phase. For example, the LC/water interface in the TEM grid was functionalized by poly(ethylene imine) conjugated to *N*-[3-(dimethylamino)-propylacrylamide].[15] The pH-dependent change in the orientation of the LCs was attributed to changes in the chain conformation at the LC/water interface, causing a change in its optical appearance. A LC biosensor made by doping 4-cyno-4-pentylbiphenyl (5CB, nematic LC at room temperature) with 4-pentylbiphenyl-4-carboxylic acid (PBA) and surface immobilization of penicillinase visualized local pH changes by the enzymatic hydrolysis of penicillin through a homeotropic-to-planar orientational change (H−P change) under polarized optical microscopy (POM) using a TEM grid cell.[16] They observed the change in the orientation of the 5CB by the small variations in pH from 7.0 to 6.9 through an enzymatic reaction. Our group also examined the TEM grid cell functionalized with pH-responsive poly(acrylicacid-*b*-4-cynobiphenyl-4-oxyundecylacrylate) (PAA-*b*-LCP) on 5CB for detecting protein and changes in pH.[13,17] The results showed that 5CB exhibited a rapid and reversible H−P change in response to the swelling and shrinkage of PAA chains by changes in the pH of the solution as well as the adsorption of protein. Therefore, the LCs can be exploited to design a label-free glucose sensor because glucose sensors normally observe a small change in pH via a glucoseoxidase (GOx) enzymatic reaction with glucose, which produces gluconic acid and decreases the local pH, as shown in Scheme 1.

Received: September 24, 2013
Accepted: November 19, 2013
Published: November 19, 2013

 © 2013 American Chemical Society

Scheme 1. GOx-Catalyzed Oxidation of Glucose

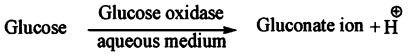

Another platform for LC biosensors is LC droplets, which can be prepared by microfluidics and emulsion techniques.[5] In response to environmental stimuli, LC droplets typically exhibit either a bipolar or radial configuration. In a bipolar configuration, LC molecules are oriented parallel to the interface of the droplet with two diametrically opposite surface-point defects, called boojums, at the poles of the droplet, whereas in the radial configuration, they are oriented perpendicular to it, with a defect at the core of the droplet. These two configurations can be distinguished from each other easily by the naked eye by POM under crossed polarizers.[18]

The present study was motivated from the previous results of the TEM grid cell functionalized with pH-responsive PAA-*b*-LCP onto 5CB for developing a glucose sensor.[17] The LCP block in PAA-*b*-LCP can penetrate easily into 5CB owing to its compatibility with LC molecules and can provide support for the PAA chains at the LC/water interface. In the present study, the flat geometry of the TEM grid cell was replaced with spherical LC droplets prepared using a microfluidics technique. LC droplets have merits over a TEM grid cell in terms of a large surface area without the need for the substrate and the housing for LC. The LC glucose sensor was fabricated by immobilizing GOx on PAA-*b*-LCP-functionalized 5CB droplets ($5CB_{PAA}$ droplets) by covalent bonds with PAA chains at the 5CB/water interface. In response to the change in pH brought on by the GOx-catalyzed oxidation of glucose, a radial-to-bipolar (R−B) orientational change occurred through a change in the PAA chain conformation. The efficiency of the 5CB droplets as a glucose sensor was demonstrated by the low production cost and simple detection of glucose from an enzymatic reaction with the naked eye.

2. EXPERIMENTAL SECTION

2.1. Materials. 5CB (TCI Japan), poly(dimethylsiloxane) (PDMS) kit (Sylgard 184, Dow Corning, USA, containing the pre-polymer and a cross-linker), poly(diallyldimethylammonium chloride) (PDDMAC) (M_w =100 000, Sigma-Aldrich), poly(sodium 4-styrenesulfonate) (PSS) (M_w = 70 000, Sigma-Aldrich), rhodamine 123 (Sigma-Aldrich), *N*-(3-dimethylaminopropyl)-N′-ethylcarbodiimide·hydrochloride (EDC·HCl) (Sigma-Aldrich), and pH buffer solutions (Samchun, Korea) were used as received. Milli-Q water (resistivity higher than 18.2 MΩ cm) was used in all experiments. Micro-slide glass (S9213, Matsunami, Japan, 76 × 52 × 1.3 mm^3) was cleaned using a hot piranha solution (H_2O_2 (35%)/H_2SO_4 (98%) 1:1 (v/v)) for 30 min followed by washing with water and drying under a nitrogen flow (*caution: piranha solution is extremely corrosive and must be handled carefully*). PAA-*b*-LCP was prepared using the same method as reported previously.[17] The molecular weight was PAA(15k)-*b*-LCP(7k) with a PDI of 1.19. The molecular weight was calculated from the GPC data of PtBA-*b*-LCP by considering 100% conversion. Supporting Information Scheme 1 presents a schematic diagram of PAA-*b*-LCP synthesis.

2.2. Device Fabrication. For the fabrication of microfluidic flow-focusing devices, PDMS was prepared by mixing the pre-polymer and the crosslinker thoroughly at the recommended ratio of 10:1 (w/w) and degassing it for 40 min in a desiccator to remove the remaining air bubbles. The final mixture was poured on a silicon wafer mold and cured inside an oven at 65 °C for 4 h before removing from the structured silicon wafer. This patterned piece of PDMS was bonded to a precleaned micro-slide glass using a short oxygen plasma treatment (46 s, Femto Science Inc., Korea). Figure SI 1 shows a schematic diagram of the microchip and dimensions of the microfluidics channel. The width of the inlet channels, the orifice width and length, and the width and height of the outlet channel were 110, 40, 40, 160, and 40 μm, respectively, and the depth throughout the channel was 100 μm. The channel walls and chip assembly were made hydrophilic by an oxygen plasma treatment. The channel was filled with water until the chip was used.

2.3. Immobilization of the GOx. LC droplet formation was carried out using the same method as reported elsewhere.[5] Briefly, the liquids were supplied to a microfluidic device via flexible plastic tubing (Norton, USA, i.d. 0.51 mm, o.d. 1.52 mm) attached to precision syringes (SGE Analytical Science, Australia) operated using digitally controlled syringe pumps (KD Scientific, KDS 100 series, USA). The flow of the fluids to the microfluidic channels was controlled using two independent syringe pumps. For 5CB/aqueous droplets formation, the continuous and dispersed phases consisted of an aqueous PAA-*b*-LCP (0.2 wt %) solution and 5CB, respectively. The continuous phase entered from the two side inlet channels, and the dispersed phase entered in the middle channel. Both phases met at the junction, and droplet formation took place when the fluids were crossing the neck of the channel. The typical flow rates used for droplet formation were 0.01 and 0.2 mL/h for the dispersed and continuous phases, respectively. The $5CB_{PAA}$ droplets were acquired in a reservoir, and the PAA chains were activated with 0.4 M EDC·HCl and 0.1 M NHS for 1 h. The $5CB_{PAA}$ droplets were kept in a GOx solution for 12 h at room temperature to obtain the GOx-immobilized 5CB droplets ($5CB_{GOx}$ droplets), as summarized in Scheme 2. The tested concentrations of the GOx solution (C_g) were 6, 9, 12, 16, 19, and 22 μM.

Scheme 2. Chemical Immobilization of the GOx to PAA

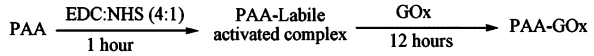

The immobilization of the GOx to the PAA was confirmed using GOx labeled with rhodamine 123 (GOx_{Rhd}), which was prepared as follows. The GOx was dissolved in PBS buffer (pH 7.2) in a reaction vial to obtain a 15.6 μM solution into which EDC·HCl (0.4 M) and NHS (0.1M) were added and kept for 1 h to activate the COOH groups of GOx. Subsequently, rhodamine (1 mg) was added, and the mixture was stirred for 12 h at room temperature. Figure SI 2 presents the UV−vis spectra of GOx_{Rhd}, GOx, and rhodamine. The spectrum of the GOx_{Rhd} showed the same strong absorbance at 500 nm as that of pure rhodamine 123 with a depression of the characteristic GOx peak at 276 nm and a blue shift to 263 nm (see arrows in Figure SI 2), indicating that labeling the GOx with rhodamine 123 was successful. The GOx_{Rhd} was then immobilized on the $5CB_{PAA}$ droplets using the same procedure. The GOx_{Rhd} solution was washed with distilled water to remove the unreacted GOx_{Rhd}, and the resulting GOx_{Rhd}-immobilized $5CB_{PAA}$ droplets ($5CB_{GOxRhd}$ droplets) were observed by a fluorescent microscope.

2.4. Measurement. The formation of on-chip droplets was imaged using an STC-TC83USB-AS camera (Sen Tech, Japan) attached to the inverted microscope. POM images of the droplets were captured using a polarized optical microscope (Leitz, ANA-006, Germany) under crossed polarizers using a CCD camera (Samwon, STC-TC83USB, Korea). The GOx_{Rhd} on the $5CB_{PAA}$ droplets was confirmed by fluorescent microscopy (Nikon Eclipse, E600POL, Japan). ^1H nuclear magnetic resonance (NMR, Bruker 400 MHz, Germany) spectroscopy of the PAA-*b*-LCP was carried out at 400 MHz. All of the experiments were carried out in a 0.2 M NaCl solution, which is almost equivalent to physiological conditions.

3. RESULTS AND DISCUSSION

3.1. Immobilization of GOx. Figures 1a shows a POM image of the $5CB_{PAA}$ droplet at pH 7 under crossed polarizers. The radial configuration corresponding to homeotropic anchoring was clearly observed. The radial droplet has the

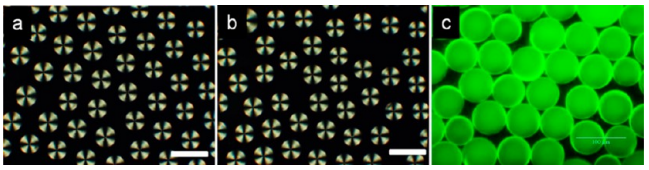

Figure 1. POM images of (a) $5CB_{PAA}$ and (b) $5CB_{GOx}$ droplets and (c) fluorescent image of the $5CB_{GOxRhd}$ droplets; the pH was 7 for these data. The scale bars in all panels are 100 μm.

most symmetrical director configuration, and the optical appearance of the droplet was invariant when viewed at differing angles by POM. The 5CB droplets without any coating were reported to have a bipolar configuration in water.[19] The R−B change by coating PAA chains on the LC droplet might be due to the charges produced by the deprotonation of carboxylic groups at pH 7; the pK_a of PAA in the bulk state is 4.7. Figure 1b shows a POM image of the $5CB_{GOx}$ droplets. The radial configuration of the droplets remained after immobilizing the GOx. To confirm the immobilization of GOx on the PAA chains, GOx_{Rhd} was immobilized on the PAA chains and observed by fluorescence microscopy, as shown in Figure 1c. The fluorescent image of the $5CB_{GOxRhd}$ droplets clearly shows a green color with a black image at the other regions, suggesting that the GOx was immobilized successfully on the PAA chains. Therefore, the long-term stability of GOx could be achieved by its immobilization through covalent bonding.

3.2. Glucose Detection. Figure 2a shows POM images of the $5CB_{GOx}$ droplets at pH 7 under the crossed polarizers after

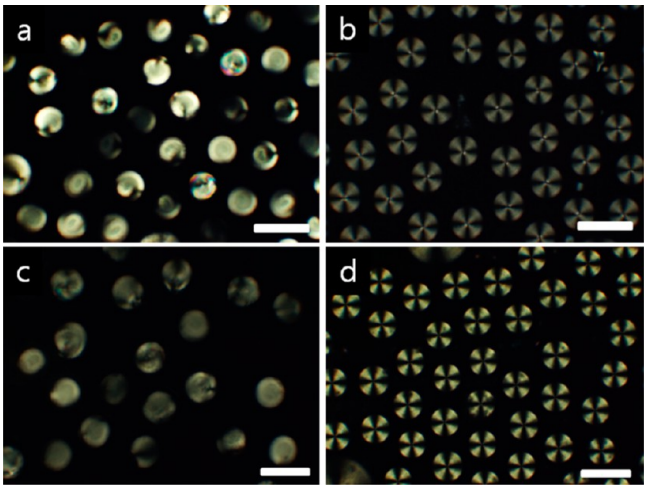

Figure 2. POM images under crossed polarizers of the $5CB_{GOx}$ droplets in (a) 1 mM glucose and (b) 1 mM galactose solutions at pH 7, and (c) PBS buffer solution at pH 2 and (d) $5CB_{PAA}$ droplets (without GOx immobiliazation) in a 1 mM glucose solution. The scale bars in all panels are 100 μm.

replacing the aqueous medium in the cell with a 1 mM glucose solution. The initial radial configuration (Figure 1b) changed to a bipolar one. This R−B change might be due to the release of H^+ ions by the enzymatic oxidation of glucose, which reduced the pH in the cell and caused protonation and shrinkage of the PAA chains. The pH-dependent shrinkage of PAA at the interface could alter the orientation of the 5CB droplets. To confirm whether the reduced pH could change the 5CB droplet, the aqueous neutral medium at pH 7 was replaced with an acidic medium at pH 2 in the container with the $5CB_{PAA}$ droplets but without the immobilization of GOx. The bipolar configuration was observed, as shown in Figure 2c, confirming that the R−B change by the addition of glucose to the $5CB_{GOx}$ droplets was due to a decrease in pH by an enzymatic reaction. Bi et al. also observed a similar H−P change in the PBA-doped 5CB confined in a penicillinase-immobilized TEM grid by the H^+ ions released from the enzymatic hydrolysis of penicillin.[16] Can the glucose solution itself alter the orientation of the 5CB droplet but not through the enzymatic reaction? To check this possibility, a 1 mM glucose solution was injected into the cell containing $5CB_{PAA}$ droplets without immobilizing GOx. The initial radial configuration did not change, as shown in Figure 2d, suggesting that this R−B change was due to the GOx-catalyzed oxidation of glucose and not the presence of glucose in the aqueous medium. The specificity of a biosensor is one of the most important considerations. The $5CB_{GOx}$ droplets were tested for two monosaccharide stereoisomers (i.e., glucose and galactose) that have different spatial arrangements of hydrogen and hydroxyl (OH) groups at carbon 4. Figure 2b shows a POM image of the $5CB_{GOx}$ droplets in response to a 1 mM galactose solution. The initial radial orientation did not change, suggesting that the $5CB_{GOx}$ droplets could detect glucose specifically against galatose despite galatose having a similar chemical structure.

3.3. Response of $5CB_{GOx}$ Droplets to Blood Solution. A blood sample of about 2 mL from a healthy donor was collected and transferred into a vial. One milliliter of blood was taken in a vial, and blood solutions of different concentrations with 10×, 100×, 250×, 500×, and 1000× dilutions were prepared. (Note that to avoid microbial activity the vials were first treated with UV for 15 min). Figure 3 shows the response of $5CB_{GOx}$

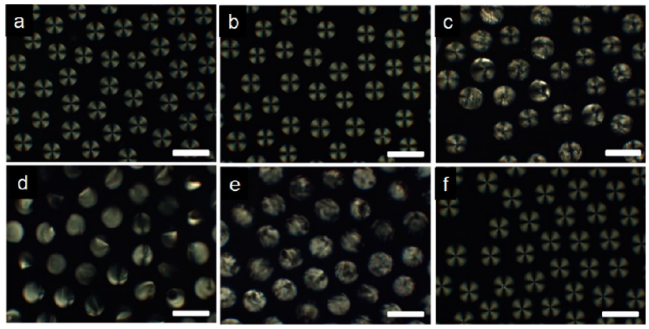

Figure 3. POM images of the $5CB_{GOx}$ droplets under crossed polarizers in a blood sample with (a) 1000×, (b) 500×, (c) 250×, (d) 100×, and (e) 10× dilutions and (f) a 0.1 wt % hemoglobin aqueous solution. The scale bars in all panels are 100 μm.

droplets to the blood samples. No R−B change was observed with the 1000× and 500× dilutions (Figure 3a,b), a slight R−B change was detected at 5 min with a 250× dilution (Figure 3c), and the R−B change became visible and all droplets changed to bipolar with the 100× and 10× dilutions (Figure 3d,e). Blood is known to contain a lot of hemoglobin in the red blood cells, which may affect the R−B change. To confirm the effect of hemoglobin on the R−B change, a 0.1 wt % hemoglobin solution was tested (Figure 3f) (0.1 wt % is higher than the concentration of the hemoglobin in the tested blood with dilution). The initial radial configuration remained, indicating that the hemoglobin did not affect the R−B orientation. Although the effects of many other components in the blood

on the R−B change should be studied, the present data suggests that the R−B change may be due to the presence of glucose in a blood solution and that $5CB_{GOx}$ droplets may provide enough specificity for prescreening glucose from the blood.

3.4. Effects of the GOx Concentration on Glucose Detection. To examine the effects of the GOx concentration on glucose detection, 2 mM glucose was injected into the cell containing the $5CB_{GOx}$ droplets immobilized with different concentrations of GOx (C_g). Figure 4a shows a POM image of the $5CB_{GOx}$ droplets immobilized at C_g = 6 μM. Only a few droplets changed from a radial to bipolar configuration with some preradial ones. When C_g was increased to 9 and 12 μM, the $5CB_{GOx}$ droplets with a bipolar configuration were more visible, as shown in Figure 4b,c. All $5CB_{GOx}$ droplets had a bipolar configuration at C_g = 16 and 19 μM (Figure 4d−f), suggesting that the immobilization density of the GOx onto the $5CB_{PAA}$ droplets was saturated at C_g = 16 μM. Therefore, all of the experiments were performed with $5CB_{GOx}$ droplets immobilized with a 16 μM GOx solution.

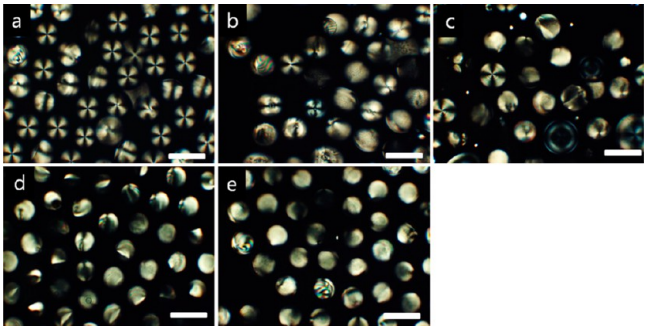

Figure 4. POM images (under crossed polarizers) of the $5CB_{GOx}$ droplets immobilized with different GOx concentrations (C_g) of (a) 6, (b) 9, (c) 12, (d) 16, and (e) 19 μM in response to a glucose solution at C_0 = 2 mM. The scale bars in all panels are 100 μm.

3.5. Sensitivity and Speed of Glucose Detection. Figure 5 shows POM images of the $5CB_{GOx}$ droplets at different concentrations (C_0) of glucose solutions. The initial radial orientation did not change at $C_0 \leq 0.02$ mM (Figure 5a−c). At C_0 = 0.006 and 0.02 mM (Figure 5b,c), the orientation of a few droplets appeared to change from a radial to preradial configuration, as marked by arrows. The preradial configuration has a single point defect with a distorted shape (the transition state during a R−B change). At $C_0 \geq 0.03$ mM (Figure 5d−i), the bipolar configuration became more evident, suggesting that the $5CB_{GOx}$ droplets detected glucose at concentrations higher than 0.03 mM under these experimental conditions. This detection limit was low compared to many other amperometric biosensors reported in the literature. For example, Zhao et al.,[20] Chu et al.,[21] Hashino et al.,[22] and Monosik et al.[23] reported detection limits of 0.058, 0.4, 0.4, and 0.96 mM with a layer-by-layer assembly of MWCNTs, poly(diethyl diallyl ammonium chloride) and poly(styrenesulponate), metal CNTs composite, CNTs with thin plasma polymerized films, and MWCNTs sandwiched between the chitosan layers, respectively. Therefore, the detection limit was lower than that of many reported glucose biosensors. This sensitive droplet system, which has a low fabrication cost, might be useful for detecting small amounts of glucose in samples by the naked eye. Figure 6a−f shows POM images of the $5CB_{GOx}$ droplets with time after injecting the 0.1 mM glucose solution (C_0 = 0.1 mM). The passage of time is denoted as t_{pass}. The initial radial droplets were still maintained at t_{pass} = 1 min, they changed to the preradial ones at t_{pass} = 2 min, and they changed to the complete radial ones at $t_{pass} \geq 5$ min. Therefore, the response time of the R−B change was several minutes for a 0.1 mM glucose concentration. This rapid detection speed also suggests that these $5CB_{GOx}$ droplets can be applied as an effective biosensor

4. CONCLUSIONS

$5CB_{GOx}$ droplets were used as a proton-sensitive glucose biosensor by coating them with PAA-*b*-LCP at the water/LC

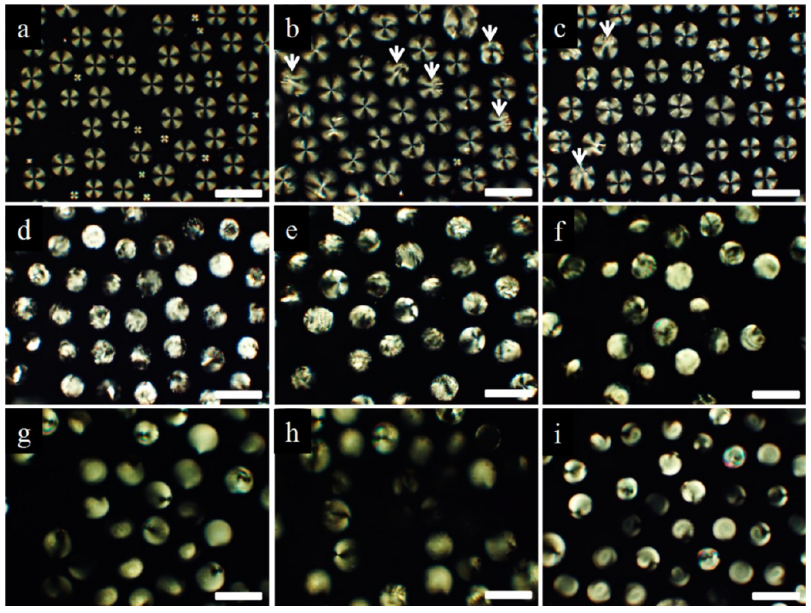

Figure 5. POM images of the $5CB_{GOx}$ droplets under crossed polarizers with different glucose concentrations (C_0) (a) 0.0006, (b) 0.003, (c) 0.02, (d) 0.03, (e) 0.05, (f) 0.15, (g) 0.3, (h) 0.5, and (i) 1 mM. The scale bars in all panels are 100 μm.

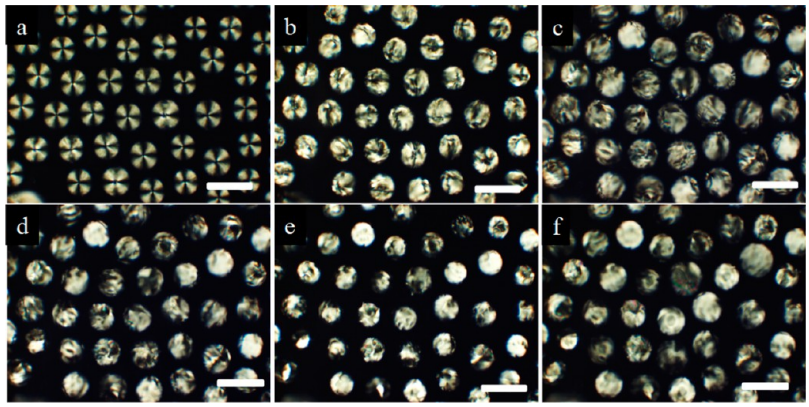

Figure 6. POM images of the $5CB_{GOx}$ droplets under crossed polarizers with times of (t_{pass}) of (a) 1, (b) 2, (c) 5, (d) 10, (e) 15, and (f) 30 min after injecting the 0.1 mM glucose solution. The scale bars in all panels are 100 μm.

interface and immobilizing GOx on the PAA chains through covalent bonding between them. This LC-based glucose biosensor could detect small amounts of glucose (0.03 mM) in a sample by the R−B change. The low detection limit of glucose, covalent bonding of GOx, short response time (several minutes), long-term stability, and selective detection of glucose against galactose suggests that these functionalized LC droplets can be used effectively as a glucose sensor with high activity and sensitivity, opening the way for their use in glucose sensing owing to the unique high sensitivity of LCs against external stimuli. Without sophisticated instruments for glucose sensing, this highly sensitive LC-based new glucose detection system is expected to allow the fabricatation of cost-effective and easy-detection (with the naked eye) glucose sensors for commercial applications.

■ ASSOCIATED CONTENT

Supporting Information

Schematic of PAA-*b*-LCP synthesis, image and schematic of the microfluidic channel with dimensions, and UV−vis spectra of the GOx labeled with rhodamine 123. This material is available free of charge via the Internet at http://pubs.acs.org.

■ AUTHOR INFORMATION

Corresponding Author

*E-mail: psy@knu.ac.kr.

Author Contributions

‡These authors contributed equally to this work.

Notes

The authors declare no competing financial interest.

■ ACKNOWLEDGMENTS

This work was supported by the National Research Foundation of Korea (NRF-2011-0020264).

■ REFERENCES

(1) Giugliano, D.; Marfella, R.; Coppola, L.; Verrazzo, G.; Acampora, R.; Giunta, R.; Nappo, F.; Lucarelli, C.; D'Onofrio, F. *Circulation* **1997**, *95*, 1783−1790.
(2) Kitabchi, A. E.; Umpierrez, G. E.; Miles, J. M.; Fisher, J. N. *Diabetes Care* **2009**, *32*, 1335−1343.
(3) Cryer, P. E.; Axelrod, L.; Grossman, A. B.; Heller, S. R.; Montori, V. M.; Seaquist, E. R.; Service, F. J. *J. Clin. Endocrinol. Metab.* **2009**, *94*, 709−728.
(4) Woltman, S. J.; Jay, G. D.; Crawford, G. P. *Nat. Mater.* **2007**, *6*, 929−938.
(5) Khan, W.; Choi, J. H.; Kimb, G. M.; Park, S. Y. *Lab Chip* **2011**, *11*, 3493−3498.
(6) Khan, W.; Seo, J.-M.; Park, S. Y. *Soft Matter* **2011**, *7*, 780−787.
(7) Kinsinger, M. I.; Buck, M. E.; Meli, M.-V.; Abbott, N. L.; Lynn, D. M. *J. Colloid Interface Sci.* **2010**, *341*, 124−135.
(8) Miller, D. S.; Abbott, N. L. *Soft Matter* **2013**, *9*, 374−382.
(9) Brake, J. M.; Mezera, A. D.; Abbott, N. L. *Langmuir* **2003**, *19*, 6436−6442.
(10) Luk, Y.-Y.; Abbott, N. L. *Curr. Opin. Colloid Interface Sci.* **2002**, *7*, 267−275.
(11) Gupta, V. K.; Skaife, J. J.; Dubrovsky, T. B.; Abbott, N. L. *Science* **1998**, *279*, 2077−2080.
(12) Jang, C. H.; Tingey, M. L.; Korpi, N. L.; Wiepz, G. J.; Schiller, J. H.; Bertics, P. J.; Abbott, N. L. *J. Am. Chem. Soc.* **2005**, *127*, 8912−8913.
(13) Seo, J. M.; Khan, W.; Park, S.-Y. *Soft Matter* **2012**, *8*, 198−203.
(14) Carlton, R. J.; Gupta, J. K.; Swift, C. L.; Abbott, N. L. *Langmuir* **2012**, *28*, 31−36.
(15) Kinsinger, M. I.; Sun, B.; Abbott, N. L.; Lynn, D. M. *Adv. Mater.* **2007**, *19*, 4208−4212.
(16) Bi, X.; Hartono, D.; Yang, K.-L. *Adv. Funct. Mater.* **2009**, *19*, 3760−3765.
(17) Lee, D. Y.; Seo, J. M.; Khan, W.; Kornfield, J. A.; Kurjib, Z.; Park, S. Y. *Soft Matter* **2010**, *6*, 1964−1970.
(18) Sivakumar, S.; Wark, K. L.; Gupta, J. K.; Abbott, N. L.; Caruso, F. *Adv. Funct. Mater.* **2009**, *19*, 2260−2265.
(19) Kinsinger, M. I.; Buck, M. E.; Abbot, N. L.; Lynn, D. M. *Langmuir* **2010**, *26*, 10234−10242.
(20) Zhao, H.; Ju, H. *Anal. Biochem.* **2006**, *350*, 138−144.
(21) Chu, X.; Duan, D.; Shen, G.; Yu, R. *Talanta* **2007**, *71*, 2040−2047.
(22) Hoshino, T.; Sekiguchi, S. i.; Muguruma, H. *Bioelectrochemistry* **2012**, *84*, 1−5.
(23) Monosik, R.; Ansky, M. S.; Luspai, K.; Magdolen, P.; Sturdik, E. *Enzyme Microb. Technol.* **2012**, *50*, 227−232.